American Journal of Botany

American Journal of Botany 100(2): 322–331. 2013.

Do ray cells provide a pathway for radial water movement in the stems of conifer trees?[1]

David M. Barnard[2,5], Barbara Lachenbruch[2], Katherine A. McCulloh[2], Peter Kitin[3], and Frederick C. Meinzer[4]

[2]Department of Forest Ecosystems and Society, Oregon State University Corvallis, Oregon 97331 USA; [3]Institute for Microbial and Biochemical Technology, USDA Forest Service, Forest Products Laboratory, One Gifford Pinchot Drive, Madison, Wisconsin 53726-2398 USA; and [4]USDA Forest Service, Forestry Sciences Laboratory, 3200 SW Jefferson Way, Corvallis, Oregon 97331 USA

- *Premise of the study:* The pathway of radial water movement in tree stems presents an unknown with respect to whole-tree hydraulics. Radial profiles have shown substantial axial sap flow in deeper layers of sapwood (that may lack direct connection to transpiring leaves), which suggests the existence of a radial pathway for water movement. Rays in tree stems include ray tracheids and/or ray parenchyma cells and may offer such a pathway for radial water transport. This study investigated relationships between radial hydraulic conductivity ($k_{s\text{-}rad}$) and ray anatomical and stem morphological characteristics in the stems of three conifer species whose distributions span a natural aridity gradient across the Cascade Mountain range in Oregon, United States.
- *Methods:* The $k_{s\text{-}rad}$ was measured with a high-pressure flow meter. Ray tracheid and ray parenchyma characteristics and water transport properties were visualized using autofluorescence or confocal microscopy.
- *Key results:* The $k_{s\text{-}rad}$ did not vary predictably with sapwood depth among species and populations. Dye tracer did not infiltrate ray tracheids, and infiltration into ray parenchyma was limited. Regression analyses revealed inconsistent relationships between $k_{s\text{-}rad}$ and selected anatomical or growth characteristics when ecotypes were analyzed individually and weak relationships between $k_{s\text{-}rad}$ and these characteristics when data were pooled by tree species.
- *Conclusions:* The lack of significant relationships between $k_{s\text{-}rad}$ and the ray and stem morphologies we studied, combined with the absence of dye tracer in ray tracheid and limited movement of dye into ray parenchyma suggests that rays may not facilitate radial water transport in the three conifer species studied.

Key words: conifers; drought; hydraulic architecture; hydraulic conductivity; radial conductivity; ray parenchyma; ray tracheids; xylem anatomy.

The bulk of water movement in tree stems occurs in the axial direction. However, water moving through inner (and anatomically older) portions of stem sapwood ultimately must move radially to reach transpiring leaves (Maton and Gartner, 2005). Despite evidence that the leaf-traces of conifers are connected only to the outer several growth rings (Maton and Gartner, 2005), stem sap flow rates have shown peaked flow in the interior layers of the sapwood, which likely do not connect directly to leaves (Phillips et al., 1996; Ford et al., 2004a, b; Domec et al., 2006). Thus, the pathway whereby water is transported from inner sapwood to transpiring leaves is unknown, and understanding this mechanism will improve our functional knowledge of whole-tree hydraulic architecture. In this study, we evaluated the role of ray tracheids and ray parenchyma in the radial transport of water in three western conifer tree species. We further examined each of these tissues in terms of its relationship with gross stem characteristics (e.g., stem diameter, sapwood depth) and radial water transport conductivity ($k_{s\text{-}rad}$; $kg \cdot m^{-1} \cdot s^{-1} \cdot MPa^{-1}$), as well as changes in these characteristics across a natural aridity gradient across the Cascade Mountain range in Central Oregon.

Radial profiles of axial sap flow vary widely among tree species and functional types (Phillips et al., 1996; Gartner and Meinzer, 2005). Douglas-fir [*Pseudotsuga menziesii* (Mirb.) Franco] has thin sapwood (15–20% of total stem diameter) and conducts the majority of its sap flow in a zone immediately adjacent to the vascular cambium (Lassen and Okkonen, 1969; Domec et al., 2006). Unlike Douglas-fir, ponderosa pine (*Pinus ponderosa* Dougl. ex Laws.) and lodgepole pine (*Pinus contorta* Dougl. ex Loudon) have thicker sapwood that comprises up to 80% of total stem diameter. The latter two species also conduct the majority of their sap flow at a distance roughly one third of the way into the active sapwood (Smith et al., 1956; Mark and Crews, 1973; Ford et al., 2004a, b). Cambial age at sapwood depths such as this can be upward of 100 yr in mature trees and would require water to traverse dozens of growth ring boundaries to flow from inner sapwood to the leaf trace connections.

Unlike axial water flow paths in tree stems, the pathway for radial water flow is poorly understood. Some tree species may conduct water radially through bordered pits on the tangential walls of the last row of axial tracheids in the latewood (Laming

[1]Manuscript received 2 July 2012; revision accepted 30 November 2012.

The authors thank Cascade Timber Consulting for supply of study material; P. Denne for discussion, B. Barnard for assistance with data collection, and D. Barnard for helpful comments. This work was supported in part by the U. S. Department of Agriculture Wood Utilization Research Special Grant to Oregon State University, by National Science Foundation (09-19871) and Joint Venture Agreement (07-JV-468) with the U. S. Department of Agriculture, Forest Service Pacific Northwest Research Station.

[5]Author for correspondence (e-mail: dave.barnard@colostate.edu); present address: Department of Horticulture and Landscape Architecture, Colorado State University, Fort Collins, Colorado 80523 USA

doi:10.3732/ajb.1200333

and Welle, 1971; Koran, 1977; Kitin et al., 2009). Other species may have semitangential pitting on axial tracheids, or radial grain, that is thought to result in obliquely radial flow (Kitin et al., 2009). However, direct radial water flow has been observed by implementing overlapping saw cuts to hydraulically isolate a section of sapwood from normal axial flow (MacKay and Weatherly, 1973). The presence of continuous radial flow (in such cases) suggests that a direct (albeit potentially transient) pathway does exist. This lack of understanding of radial pathways notwithstanding, several physiological studies have sought to assess the importance of radial water movement (James et al., 2003; Domec et al., 2005, 2006; Kitin et al., 2009; Barnard et al., 2011).

Rays in conifer stems can be comprised of ray parenchyma and/or ray tracheid cells. Ray parenchyma cells are living at maturity and play a role in heartwood formation (Bamber, 1976; Spicer, 2005), storage and transport of assimilates (Sauter and van Cleve, 1994; Gartner et al., 2000; Fuchs et al., 2010) and in a variety of processes linked to wounding and mechanical padding (reviewed in Gartner, 1995). Ray tracheids are found only in certain genera of woody species, are dead at maturity, and have cell walls that tend to be thicker and more highly lignified than those of ray parenchyma (Singh et al., 2006).

Resistance to water movement would differ if the pathway were through cells of ray tracheids compared with ray parenchyma or both together. Because ray parenchyma cells are connected to axial tracheids by cross-field (half-bordered) pits (Coté and Day, 1969; Panshin and de Zeeuw, 1980; van Bel, 1990) they may offer a radial flow path for water. However, there would be significant hydraulic resistance to water movement from an axial tracheid into a ray parenchyma cell from the shared pit membrane at the cross-field pit. Assuming this resistance was overcome, water could then move through plasmodesmata or aquaporins from cell to cell in the radial direction. In contrast, ray tracheids are connected to other ray and axial tracheids by bordered pit pairs, which are the same pit type that connects adjacent axial tracheids to enable water movement (Gordon, 1912; Coté and Day, 1969). While ray tracheids are generally small in diameter, they may provide a pathway with less hydraulic resistance than ray parenchyma. Transmission electron micrographs of ray tracheids in southern yellow pine (*Pinus* spp.) show a torus-margo pit membrane complex similar to that in axial tracheids (Coté and Day, 1969), which suggests that ray tracheids play a role in xylem safety and efficiency.

Climate and vegetation are different on the west and east sides of the crest of the Cascade Mountains in Oregon. The west side has high precipitation (1000–3000 mm·yr^{-1}) and a relatively narrow temperature range (given the latitude) as a result of the maritime influence of the Pacific Ocean. The east side of the Cascade Crest experiences low precipitation (100–300 mm·yr^{-1}) and a more continental climate with cold winters with frozen precipitation and warm and dry summers. Despite these differences, the native ranges of several tree species extend into both climate regimes. Douglas-fir, for example, is a dominant canopy species on both sides of the Cascade Crest but has one variety native to the west side (*P. meinziesii* var. *meinziesii*) and another to the east side (*P. meinziesii* var. *glauca*) (Burns and Honkala, 1990). Similarly, shore pine (*P. contorta* var. *contorta*) is a coastal subspecies of the intermountain-west lodgepole pine (*P. contorta* var. *murrayana*), whereas ponderosa pine (the most widely distributed pine in North America [Burns and Honkala, 1990]), is represented in the Willamette Valley, west of the Cascade Crest, by a genetically distinct ecotype. The difference in climatic factors east and west of the Cascade Crest and the presence in each of genetically distinct ecotypes of tree species provides an opportunity to study variation in structural and functional features of sapwood that may be adaptive for maintaining water transport under contrasting conditions.

The objective of this research was to determine the existence of radial apoplastic flow pathways in three conifer species in two contrasting habitats in the western USA. To do this, we studied the relationship(s) between sapwood $k_{s\text{-}rad}$ and selected morphological parameters in each tree species and the relationship of these parameters to xylem ray anatomy. Based on Darcy's law, which stipulates that less driving force (xylem tension in this case) is required for a given rate of flow across a larger (compared with smaller) cross-sectional area (assuming constant conductivity), we hypothesized that ecotypes from the east side of the Cascade Crest would have thicker sapwood than western ecotypes. Second, we hypothesized that sapwood thickness would be correlated with $k_{s\text{-}rad}$, given that under the same pressure gradient high $k_{s\text{-}rad}$ would allow access to water deeper within the sapwood. Finally, we hypothesized that ecotypes with a high ray tracheid-to-ray parenchyma ratio have high $k_{s\text{-}rad}$ because ray tracheids offer a comparatively low resistance pathway for sap flow.

MATERIALS AND METHODS

***Site characteristics and sample material*—**We studied *Pinus contorta* Douglas ex Loudon, *Pinus ponderosa* Douglas ex Laws., and *Pseudotsuga menziesii* ex Mirb. because all three species have ray tracheids but differ in sapwood thickness and ray tracheid size and frequency. The presence of distinct ecotypes of each species on the east and west sides of the Cascade Crest allowed us to investigate the effect of climate on of apoplastic flow pathways and stem characteristics among and between genotypes. Hereafter, we use "eastern" and "western" to denote the ecotypes of each tree species that occur on the east or west side, respectively, of the Cascade Crest. Because the common names of the eastern and western ecotypes of *Pinus contorta* differ (lodgepole pine and shore pine, respectively), we instead refer to them as eastern or western lodgepole.

We sampled two stands each of each tree species (12 stands total) on the eastern and western sides of the Cascade Crest) in central and western Oregon (Table 1). Within each stand, 12 trees were sampled (N = 144) each with a breast-height (1.3 m) diameter of 20–40 cm. All trees selected in each stand had similar crown sizes, were vigorous, and of healthy appearance (i.e., lacking visible damage or insect or disease infestation). For each tree, we measured sapwood depth, the number of sapwood rings and tree age by extracting two different 5-mm-diameter increment cores, each at approximately 1.3 m above ground level. Cores were taken at 90° angles to one another from trees growing on relatively flat ground and without visible trunk curvature or lean. For trees that had trunk curvature or lean or for those growing on a slope, we took cores at 180° to one another and 90° from the axis of lean in an effort to avoid compression and opposite wood.

Measurements of $k_{s\text{-}rad}$ (described later) were collected from separate 12.5-mm-diameter increment cores extracted at breast height from six trees randomly selected from among the 12 trees described. Each core was taken from a location that minimized the presence of compression or opposite wood. If sapwood depth was ≤3 cm (i.e., western Douglas-fir), we took three cores to ensure sufficient sample material. Otherwise, only two cores were extracted. We marked the heartwood–sapwood boundary of each core (according to a change in translucency) with a pencil. Each core was placed inside a plastic bag, which was sealed and labeled according to the sample number. This bag was sealed inside a second plastic bag that was placed into an ice-filled cooler for transport to the laboratory.

***Radial conductivity ($k_{s\text{-}rad}$)*—**Each 12.5-mm-diameter increment core was cut into 10-mm-long segments (extending in the radial direction). These segments corresponded to outer, middle, and inner sapwood. The outer segment

TABLE 1. Stand locations and site characteristics from which samples were collected. Mean annual precipitation and maximum and minimum temperatures are data from nearest city in Oregon, United States.

Location	Species sampled	No. of stands	Nearest city	Latitude (°N), Longitude (°W)	Elevation (m asl)	General site characteristics	Annual precip. (mm)	Annual max./ min. temp (C°)
Eastern sites								
Ochoco National Forest	Douglas-fir	2	Mitchell	43.584, −121.218	1185	(1) 20° Slope and (2) flat area, both with mixed Douglas-fir and ponderosa pine	290	30 / −4
Sand Springs	Lodgepole pine	1	Milican	43.627, −120.858	1645	Pure lodgepole pine stand, flat area adjacent to volcanic butte	285	29 / −4
Pine Mountain	Ponderosa and lodgepole pine	2	Milican	43.767, −120.963	1400	Mixed ponderosa and lodgepole pine at flat desert fringe area	300	27 / −4
Deschutes National Forest	Ponderosa pine	1	La Pine	43.584, −121.218	1680	Pure ponderosa pine stand, flat area	260	29 / −4.5
Western sites								
MacDonald-Dunn	Douglas-fir	1	Corvallis	44.616, −123.293	200	Mixed stand of Douglas-fir, big leaf maple and grand fir, flat area	1110	28 / 1
Seal Rock	Lodgepole pine	1	Waldport	44.496, −124.083	30	Mixed stand of lodgepole pine and Sitka spruce	2300	25 / 2.5
Gleneden	Lodgepole pine	1	Depoe Bay	44.876, −124.036	10	Pure lodgepole pine stand	2210	25 / 2.0
Cascade Timber Consulting	Ponderosa pine and Douglas-fir	3	Sweet Home	44.368, −122.828	285	(1) Pure ponderosa pine stand, (2) Mixed ponderosa pine and Douglas-fir, (3) Mixed Douglas-fir, big leaf maple and grand fir	1390	27 / 0.5

boundary was considered to begin at the third growth ring inward from the vascular cambium to preclude the presence of immature cells from the cambial zone. The middle segments were centered one-half the distance between the vascular cambium and the heartwood–sapwood boundary. The inner segment was considered to end at the second growth ring outward from the heartwood–sapwood boundary to ensure no heartwood was included in the sample. The fresh mass and volume (determined by the immersion method [below]) of each sample was recorded, and all samples were placed into a perfusion solution that contained filtered (0.22 μm) and degassed, distilled water adjusted to pH 2 with HCl to retard bacterial and fungal growth (Cochard, 1992; Maherali and DeLucia, 2000). The samples were infiltrated with water under partial vacuum overnight to remove any gas embolisms. Radial conductivity ($k_{s\text{-}rad}$) was determined using the high pressure flowmeter (HPFM) method described by Tyree et al. (1993) and Yang and Tyree (1994). Radial conductivity was calculated based on the pressure drop observed across a capillary tube of known resistance located between the sample and a pressurized tank. Capillary tube resistance was determined previously by recording pressure differential (MPa) and flow rate ($kg \cdot s^{-1}$). Calibration curves derived from these data were used to determine flow rate (f) through the sample ($kg \cdot s^{-1}$) at a given pressure differential (MPa). The pressure gradient (ΔP; $MPa \cdot m^{-1}$) was thus calculated as

$$\Delta P = \frac{p_{u\text{-}s}}{l}, \quad (1)$$

where $p_{u\text{-}s}$ is the pressure (MPa) at the upstream end of the capillary tube and l is the length (m) of the sample. Pressure gradient and flow rate were then used to calculate hydraulic conductivity (k_h; $kg \cdot m \cdot s^{-1} \cdot MPa^{-1}$) as

$$k_h = \frac{f}{\Delta P}. \quad (2)$$

Hydraulic conductivity was normalized according to sample cross-sectional area (A; estimated as πr^2 for the 12 mm-diameter increment core) and the specific conductivity (k_s; $kg \cdot m \cdot s^{-1} \cdot MPa^{-1}$) calculated according to the following equation:

$$k_s = \frac{k_h}{A}. \quad (3)$$

Preliminary studies showed that $k_{s\text{-}rad}$ decreased with increasing pressure until the pressure differential approached 0.12 MPa at which point there was no further decrease in $k_{s\text{-}rad}$. On the basis of this work, we perfused samples for 10–15 min at a pressure of 0.15 MPa.

***Sample density and growth ring properties*—**Core volumes of the hydraulics samples were estimated (see density calculations later) by immersing each sample in water on a balance and recording the volume of water displaced. We counted the number of growth ring boundaries (i.e., the latewood from a previous year to the earlywood of the next year) with a tree-ring measuring device (Metronics QC10-V, Metronics, Bedford, New Hampshire, USA). We then oven-dried each sample at 70°C (Thelco 17, Thelco Corp., Englewood, Colorado, USA) until there was no measurable change in mass and recorded this value for the later determination of sample density (dry mass per green volume, $g \cdot cm^{-3}$).

***Ray characteristics, proportions, and anatomy*—**We cut 30-μm-thick tangential sections of outer sapwood using a sliding microtome. Unstained sections were mounted in glycerin and analyzed with a fluorescence microscope and the UV-2A filter (Nikon Eclipse E400, Nikon, Melville, New York, USA). The lignified walls of the ray tracheids for all samples autofluoresced as bright blue, whereas the walls of the ray parenchyma cells fluoresced as dark blue. We recorded one 10× image (about 1.25 mm^2) for each sample using a microscope-mounted digital camera (Micropublisher 5.0 RTU, QImaging, Surrey, B.C., Canada) and Q Capture Pro imaging software (QImaging Canada). To select an image, we inspected the entire section for an area of acceptable resolution then recorded one image from this area. We used ImageJ (National Institutes of Health, Bethesda, Maryland, USA) image analysis software to measure the ray tracheid and ray parenchyma lumen areas for the image from each slide from each of the 144 trees that were sampled. Individual ray cells overlapping the edge of the digital image were excluded from measurement, whereas we counted all ray cells in the image including those overlapping its edge.

Measurements from the images were used to calculate mean lumen diameters of ray tracheids and ray parenchyma, the percentage of total tangential area occupied by each cell type, and the frequency of cells per square millimeter of image area. In addition, we calculated the percent of total tangential area consisting of ray lumen and the total ray frequency per square millimeter of image area.

***Dye-flow experiments and microscopy*—**Two 12.5-mm cores were collected from each of three Douglas-fir trees from the MacDonald-Dunn Forest research site (Table 1) and were brought to the laboratory as described earlier in the method of $k_{s\text{-}rad}$ measurements. A 2-cm-long segment of the outer sapwood was cut under water from each core and water-saturated under partial

vacuum to remove air-embolisms. The side walls of the cores were wrapped with Parafilm to seal open axial tracheids and heat-shrink tubing fitted tightly around the cores as an outermost layer. In this way, only tangential faces of the water-saturated cores were left unsealed. A 0.2% (w/v) acid fuchsin solution (which moves through woody xylem similar to water [Sano et al., 2005; Umebayashi et al., 2007]) was pulled through each sapwood core for 10 min at a pressure of −5 to −6 kPa, and the core was then snap-frozen in liquid nitrogen. Cryofixed cores were stored at −12°C. Radial and tangential sections were cut from the frozen cores using a precooled razor blade and stored immediately in liquid nitrogen. Each section was observed at −30°C with an epifluorescence microscope (Nikon E400) as described by Kitin et al. (2010). Images were recorded with a digital CCD camera (Q Imaging, Micropublisher 5.0 RTV). Some replicates of the cryocut sections were freeze-dried and observed at room temperature with the epifluorescence microscope (emission filters LP 420 and LP 520) or a confocal microscope (LSM, Carl Zeiss 510) using two-channel imaging with 488 and 543 laser lines, emissions BP500–530 and LP590 nm.

The histological structure of rays was observed in 20-μm-thick radial sections of sapwood from Douglas fir, ponderosa pine, and lodgepole pine and differentiated via safranin-staining or by confocal microscopy for unstained samples as described earlier.

***Data analysis*—**There were no significant differences between ecotypes of each species from the eastern and western sites ($P > 0.20$ [one-way ANOVA; data not shown]). Consequently, data from the eastern and western sites were pooled by ecotype. The resulting pools comprised $N = 24$ individuals for growth characteristics and $N = 12$ individuals for water transport and anatomical characteristics. We used ANOVA with Tukey's honestly significant difference (HSD) test for means separation and linear regression procedures for correlation analysis. A significance level of 5% was used throughout. All statistical tests were made using S Plus (TIBICO Software, Palo Alto, California, USA)

RESULTS

***General growth characteristics*—**Eastern and western ecotypes of ponderosa pine had the largest sapwood thickness of all species and ecotypes sampled (Table 2). Sapwood was significantly thicker in eastern ecotypes of lodgepole pine ($F_{5,141} = 5.31$, $P < 0.001$) and Douglas-fir ($F_{5,141} = 2.99$, $P = 0.013$) than in their western counterparts but not in ponderosa pine ($F_{5,141} = 1.34$, $P = 0.25$). The number of growth rings in the sapwood of eastern ecotypes was significantly higher than western ecotypes in all three tree species ($F_{5,141} > 5$, $P < 0.001$, Table 2). Sapwood density ($g \cdot cm^{-3}$) was higher in western ecotypes than eastern ecotypes of ponderosa pine ($F_{5,141} = 6.74$, $P < 0.001$; Table 2) but not significantly different in eastern and western lodgepole pine or Douglas-fir ($F_{5,141} = 1.11$, $P = 0.36$ and $F_{5,141} = 0.61$, $P = 0.69$ respectively).

***Radial conductivity and dye experiments*—**There was no significant variation in $k_{s\text{-}rad}$, across sapwood depths, except for western ecotypes of ponderosa pine and lodgepole pine. These species showed opposing patterns of $k_{s\text{-}rad}$ with sapwood depth (Fig. 1, Table 3). Values of $k_{s\text{-}rad}$ ranged from 2.25×10^{-3} $kg \cdot m^{-1} \cdot s^{-1} \cdot MPa^{-1}$ in eastern Douglas-fir up to 3.46×10^{-3} $kg \cdot m^{-1} \cdot s^{-1} \cdot MPa^{-1}$ in western Douglas-fir. Eastern ecotypes of all species had significantly lower $k_{s\text{-}rad}$ than did western ecotypes ($F_{5,65} = 4.05$, $P = 0.003$, Table 3). Dye tracer experiments in Douglas-fir showed no visible infiltration into ray tracheids (Fig. 2A, B) but did show dye infiltration into the ray parenchyma (Fig. 2A, B, E) and axial tracheids (Fig. 2C, D). The dye experiments also showed that growth ring boundaries appear to present a substantial obstacle to radial flow in Douglas-fir (Fig. 2D).

***Ray cell lumen area and cell wall characteristics*—**Average lumen area of ray tracheids ranged from 57.4 μm^2 in western Douglas-fir to 211 μm^2 in western lodgepole pine (Table 3). There was no significant difference in the average area of ray tracheid lumens ($F_{5,65} = 1.39$, $P = 0.24$) between eastern and western ecotypes for any tree species (Table 3). Differences in ray parenchyma lumen areas were not significant between eastern and western ecotypes of Douglas-fir ($F_{5,65} = 0.68$, $P = 0.64$) or ponderosa pine ($F_{5,65} = 0.48$, $P = 0.79$), but ray parenchyma were significantly larger in western compared with eastern lodgepole pine ($F_{5,65} = 3.87$, $P = 0.004$, Table 3).

The mean lumen areas of ray parenchyma from eastern lodgepole pine were larger than those of ponderosa pine ($F_{5,65} = 3.49$, $P = 0.007$), which were larger than those of Douglas-fir ($F_{5,65} = 2.71$, $P = 0.028$, Table 3). Mean ray parenchyma lumen areas were also larger in western lodgepole pine than in Douglas-fir ($F_{5,65} = 3.49$, $P = 0.007$) but not ponderosa pine ($F_{5,65} = 2.09$, $P = 0.078$), whereas ray parenchyma lumen areas in the latter two species were not statistically different ($F_{5,65} = 1.64$, $P = 0.16$, Table 3).

Total ray frequency was significantly higher in eastern ecotypes of all species ($F_{5,65} > 5$, $P < 0.001$), was highest in eastern Douglas-fir, lowest in western lodgepole pine and varied significantly among all species ($F_{5,65} > 5$, $P < 0.001$, Table 3). The percentage of total tangential area comprised of ray lumen area (the sum of the percentage lumen area of ray tracheids and of ray parenchyma) was highest in the eastern ecotype of Douglas-fir ($F_{5,65} = 2.4$, $P = 0.046$), but differences were not significant between ecotypes of ponderosa pine ($F_{5,65} = 0.41$, $P = 0.84$) and lodgepole pine ($F_{5,65} = 1.31$, $P = 0.27$, Table 3). Overall, lodgepole pine had significantly higher ($F_{5,65} > 5$, $P < 0.001$) percentage of total ray lumen area than Douglas-fir and ponderosa pine, which did not differ significantly from each another ($F_{5,65} = 1.15$, $P = 0.34$).

The percentage of total tangential area that was ray tracheid lumen area was significantly higher in eastern ecotypes ($F_{5,65} > 5$,

TABLE 2. General tree growth characteristics from east- and west-side ecotypes of the three species studied. Values indicate mean ± SE ($N = 12$ for sapwood density and $N = 24$ for other characteristics). Different letters in a column indicate statistical significance at $P = 0.05$.

Location	Sapwood thickness (cm)	DBH (cm)	Age (years)	Rings of sapwood (no.)	Growth rate ($cm \cdot year^{-1}$)	Sapwood density ($g \cdot cm^{-3}$)
Eastern sites						
Douglas-fir	3.3 ± 0.2a	37.7 ± 0.7a	101.4 ± 2.9a	31.5 ± 1.6a	0.37 ± 0.01a	0.49 ± 0.01a
Ponderosa pine	12.9 ± 0.4b	39.4 ± 1.0a	80.5 ± 4.2b	68.6 ± 2.5b	0.50 ± 0.03b	0.39 ± 0.01b
Lodgepole pine	5.2 ± 0.2c	31.6 ± 1.0b	85.0 ± 3.8b	41.2 ± 3.8c	0.38 ± 0.01c	0.39 ± 0.01b
Western sites						
Douglas-fir	2.5 ± 0.3a	33.7 ± 0.8b	61.1 ± 2.2c	9.6 ± 0.8d	0.56 ± 0.02d	0.50 ± 0.01a
Ponderosa pine	12.1 ± 0.5b	37.4 ± 0.4a	51.2 ± 1.7d	42.6 ± 1.8e	0.74 ± 0.03e	0.48 ± 0.01c
Lodgepole pine	2.4 ± 0.2c	27.0 ± 1.2c	41.5 ± 2.1e	13.4 ± 1.0f	0.66 ± 0.03f	0.41 ± 0.01b

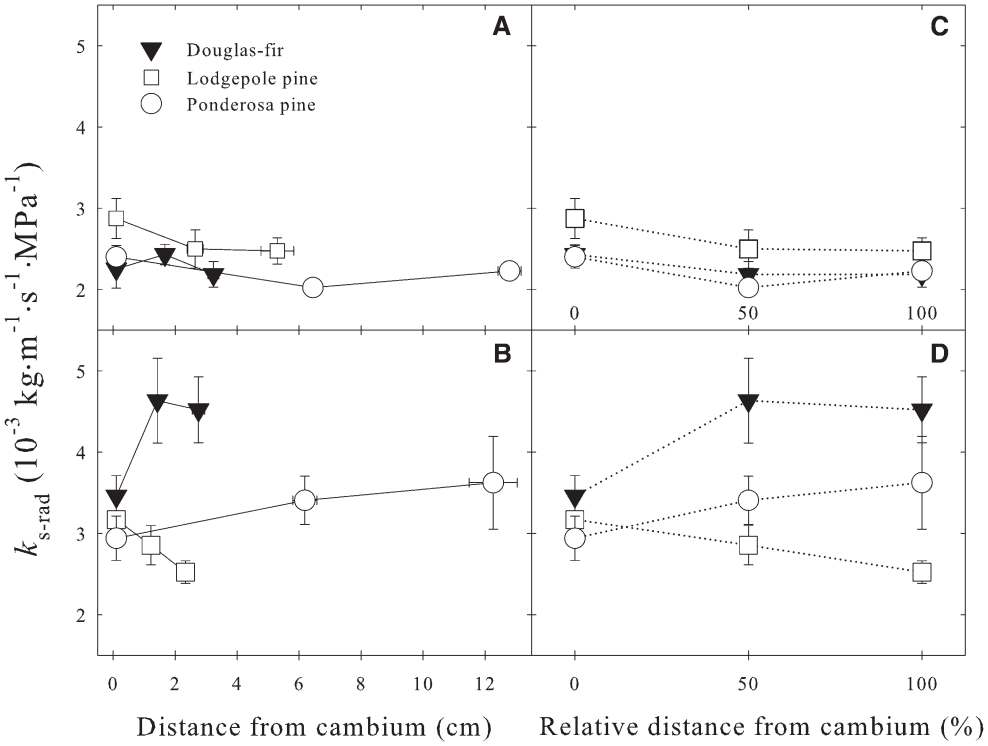

Fig. 1. Sapwood radial conductivities of east side (upper panels) and west side (lower panels) for (list the species). Panels A and B represent radial conductivities in relation to absolute sapwood depths; panels C and D represent conductivities at relative sapwood depths. Error bars represent one standard error ($N = 12$).

$P = 0.001$, Table 3) and ranged from 0.4% in Douglas-fir up to 3.2% in lodgepole pine. Ray parenchyma percentage of total area was significantly higher in eastern Douglas-fir than ponderosa pine and lodgepole pine ($F_{5,65} > 5$, $P < 0.001$, Table 3) but ponderosa pine and lodgepole pine were not significantly different ($F_{5,65} = 1.69$, $P = 0.15$). Ray parenchyma percentages of total area in western ecotypes of each species were not statistically different ($F_{5,65} = 1.09$, $P = 0.37$). Differences in ray parenchyma percentages between eastern and western ecotypes were not significant for any species ($F_{5,65} = 0.61$, $P = 0.69$, Table 3).

The frequency of ray tracheids (no. of tracheids per millimeter of total area) was significantly higher in the east-side ecotypes of all three species ($F_{5,65} > 5$, $P < 0.001$, Table 3). Ray tracheid frequency did not differ significantly between lodgepole pine and ponderosa pine in either eastern ($F_{5,65} = 1.13$, $P = 0.35$) or western ($F_{5,65} = 1.38$, $P = 0.24$) ecotypes, but was significantly lower in east-side and west-side varieties of Douglas-fir ($F_{5,65} > 5$, $P < 0.001$ for both). Ray parenchyma frequency was significantly higher in the eastern ecotype of Douglas-fir ($F_{5,65} > 5$, $P < 0.001$, Table 3) than the western ecotype, whereas western ray parenchyma frequency was higher in western ponderosa pine ($F_{5,65} = 4.29$, $P = 0.002$). Ray parenchyma frequency was statistically different among eastern and western ecotypes of the three species ($F_{5,65} > 5$, $P < 0.001$ for both comparisons).

Ray tracheids in all three species had relatively thick cell walls (Fig. 3A–C). Ray parenchyma cells in ponderosa pine and Douglas-fir were relatively thin-walled (Fig. 3A, B), whereas cell walls of ray parenchyma in lodgepole pine appeared thicker and more lignified (Fig. 3C). Ray parenchyma in the sapwood contain living nuclei and protoplasts (Fig. 3A).

TABLE 3. Radial conductivity ($k_{s\text{-}rad}$) and ray properties. Values of $k_{s\text{-}rad}$ for outer, middle, and inner sapwood sections along with ray tracheid (RT) and ray parenchyma (RP) characteristics (of outer samples) in eastern and western ecotypes of Douglas-fir, ponderosa pine and lodgepole pine. Differing letters in a column indicate statistical significance at $P = 0.05$. Values represent mean ± SE ($N = 12$).

Location	$k_{s\text{-}rad}$(10^{-3} kg·m^{-1}·s^{-1}·MPa^{-1})			Ray frequency (no.·mm^{-2})	Mean RT lumen area (μm^2)	Mean RP lumen area (μm^2)	RT % of total area	RT frequency (no.·mm^{-2})	RP % of total area	RP frequency (no.·mm^{-2})
	Outer	Middle	Inner							
Eastern sites										
Douglas-fir	2.25 ± 0.2a	2.43 ± 0.1a	2.19 ± 0.2a	33.5 ± 0.6a	60.1 ± 1.1a	210 ± 1.6a	0.4 ± 0.0a	65.0 ± 1.8a	3.8 ± 0.4a	192 ± 10.2a
Ponderosa pine	2.40 ± 0.1a	2.02 ± 0.1a	2.23 ± 0.1a	29.5 ± 0.8a	130 ± 4.7b	284 ± 16b	2.3 ± 0.1b	126 ± 6.4b	1.8 ± 0.1b	64.7 ± 3.3b
Lodgepole pine	2.87 ± 0.3a	2.50 ± 0.2a	2.47 ± 0.2a	26.1 ± 0.8a	210 ± 3.2c	376 ± 31c	3.2 ± 0.1c	127 ± 3.4b	2.3 ± 0.1c	63.8 ± 2.3b
Western sites										
Douglas-fir	3.46 ± 0.25b	4.63 ± 0.5b	4.52 ± 0.4b	28.1 ± 0.9b	57.4 ± 2.3a	230 ± 15a	0.4 ± 0.0a	57.5 ± 2.6a	2.2 ± 0.1d	131.7 ± 8c
Ponderosa pine	2.94 ± 0.27b	3.41 ± 0.3c	3.62 ± 0.6c	25.4 ± 0.9b	103 ± 9.1b	270 ± 15b	1.8 ± 0.0d	94.9 ± 5.5c	2.9 ± 0.6e	83.3 ± 4.3d
Lodgepole pine	3.17 ± 0.17b	2.85 ± 0.2d	2.52 ± 0.1d	23.1 ± 0.6d	211 ± 7.0c	510 ± 19d	2.7 ± 0.2e	97.3 ± 3.5c	3.2 ± 0.6f	69.3 ± 5.4e

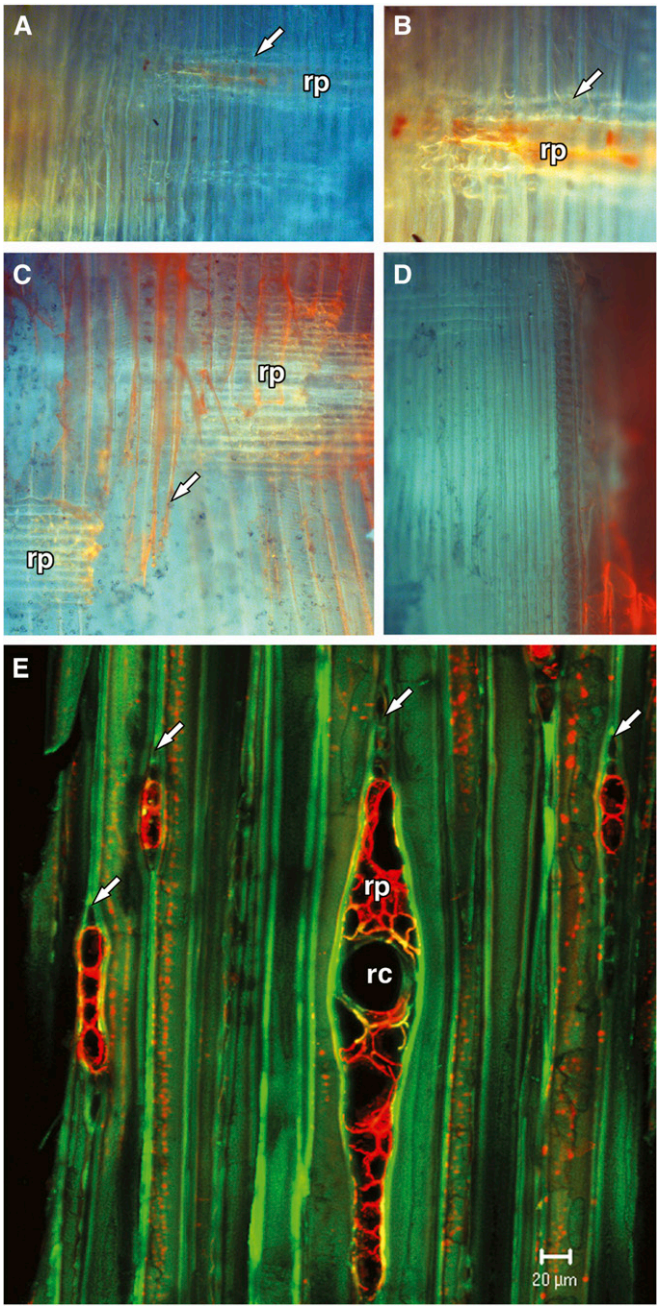

Fig. 2. Movement of aqueous acid fuchsin in the sapwood of Douglas-fir under a radial pressure gradient. Conducting cells are stained in red in panels A–D, images are of frozen radial sections and wide-field cryo-fluorescence microscopy. (A) General view of a radial section showing movement of the dye in ray parenchyma (rp) but not in ray tracheids (rt) (arrow). (B) Detail of the same section shown in panel (A). (C) Movement of the dye in axial tracheids and acid fuchsin bound to cell walls (red color, arrow). (D) Stained earlywood and unstained latewood and that the radial distribution of the dye is limited because of a higher resistance to the radial apoplastic flow at growth-ring boundaries and latewood tracheids. Panel E is a freeze-dried tangential section imaged with confocal microscopy that was cut 2–3 mm apart from the stained axial tracheids and shows that the dye is transported through ray parenchyma but did not fill ray tracheids and resin canals.

Relationships of anatomy and growth characteristics with $k_{s\text{-}rad}$—There was a significant relationship between $k_{s\text{-}rad}$ and ray tracheid frequency in eastern Douglas-fir and average ray tracheid lumen area in western ponderosa pine; differences in all other comparisons were not significant (Table 4). The number of growth rings in the conductivity samples was significantly correlated with $k_{s\text{-}rad}$ in western ecotypes of ponderosa pine (Table 5), but all other correlations were not significant. However, when data for all ecotypes of all species were pooled, significant relationships were evident between $k_{s\text{-}rad}$ and tree age ($P = 0.003$), diameter at breast height ($P = 0.03$), annual average basal growth rate ($P = 0.03$), and number of growth rings included in conductivity sample ($P = 0.004$, Table 6). None of the pooled comparisons of $k_{s\text{-}rad}$ with ray characteristics were significant ($P > 0.05$; Table 6).

DISCUSSION

We found inconsistent or nonsignificant relationships between $k_{s\text{-}rad}$ and ray tracheid and ray parenchyma parameters or stem morphological characteristics. We also found a lack of dye infiltration into ray tracheids in Douglas-fir stem wood along with limited dye infiltration into ray parenchyma. These results are surprising given that ray tracheids have been assumed to function in the radial transport of water (Tyree and Zimmermann, 2002) and that direct radial water movement does occur (MacKay and Weatherly, 1973). The lack of consistent relationships, whether at the ecotype (cf. Tables 4, 5) or pooled sample analysis level (Table 6), suggests that some alternative suite of anatomical or physiological traits may have greater control on $k_{s\text{-}rad}$ than ray cells. We also found inconsistent inter- and intraspecific differences in trends of $k_{s\text{-}rad}$ (Fig. 1). Taken as a whole, these results emphasize the need for further investigation of possible alternative pathways of radial water movement in the xylem.

Despite the lack of a strong relationship between $k_{s\text{-}rad}$ and ray anatomical characteristics in this study, literature reports suggest that a direct radial pathway may exist (MacKay and Weatherly, 1973). A direct pathway would have to bypass the resistance of growth ring boundaries or be driven by a strong enough pressure gradient to overcome such resistance. Interestingly, radial tension gradients can be up to 100 times greater than axial tension gradients (Domec et al., 2006) and could serve as the driving force for water transport through novel or otherwise unanticipated pathways. For example, water transport through ray parenchyma would require water to cross the semipermeable membrane of cross-field pits and would offer a resistance that presumably is absent in tracheary cells. However, the presence of membrane-bound proteins (e.g., aquaporins) has been shown to facilitate and regulate water flow and could have implications for water storage and release in the sapwood (Chrispeels and Maurel, 1994; DeBoer and Volkov, 2003; Lovisolo and Schubert, 2006). Microscopic inspection of Douglas-fir sapwood in the present study showed that the end walls of ray tracheids are not consistently connected by bordered pits or, if the pits are present, that they may be small with very low apparent conductivities (Fig. 3B, C). If the latter case is true our investigation of ray tracheid lumen area alone may not have fully characterized the contribution of radial conductivity attributable to ray tracheids.

The decrease in radial conductivity with increasing number of growth ring boundaries from the pooled ecotypes (Table 6),

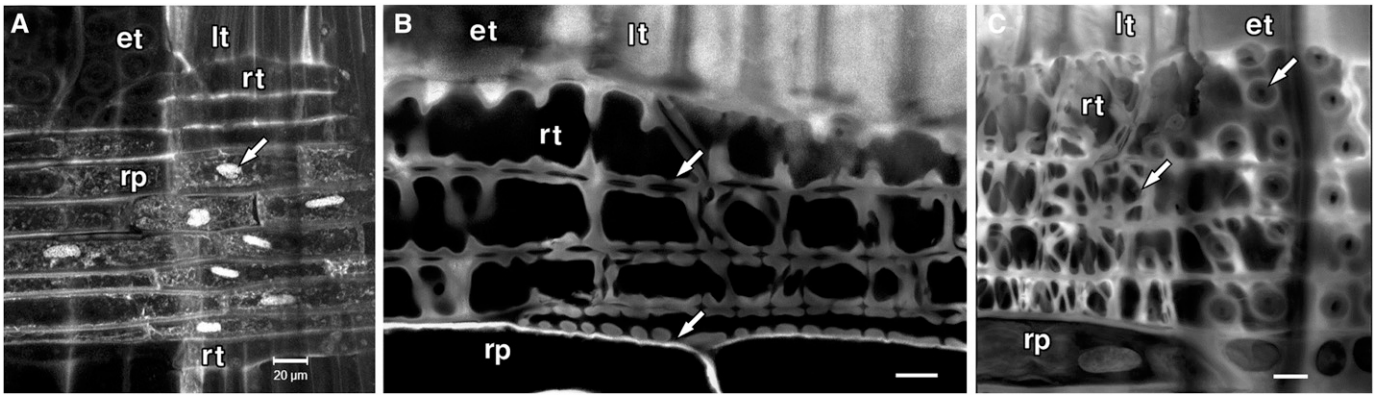

Fig. 3. Structure of xylem rays in radial sections of sapwood visualized by confocal microscopy. (A) Ray tracheids (rt), ray parenchyma (rp), and boundary between earlywood tracheids (et) and latewood tracheids (lt) in Douglas-fir. Ray parenchyma cells are thick-walled with nuclei and protoplasts. (B) Thin-walled, nonlignified ray parenchyma and thick-walled ray tracheids in ponderosa pine. The upper arrow shows ray tracheid to ray tracheid bordered pits and the lower arrow shows pits between ray tracheids and ray parenchyma. (C) Lodgepole pine with thick-walled ray parenchyma and short and thick-walled ray tracheids. The upper arrow shows earlywood tracheid to ray tracheid bordered pits (outer side of the earlywood tracheid cell wall); lower arrow shows ray tracheid-to-latewood tracheid bordered pits (inner side of the ray tracheid wall).

suggests that a significant resistance to radial water flow occurred at the growth ring boundaries or near the transition to latewood. This negative correlation, in the absence of other correlated variables, suggests that the resistance encountered by growth ring boundaries may be the main determinant of $k_{s\text{-}rad}$ and that the primary pathway for apoplastic radial flow is independent of the rays themselves.

Given the dimensions of the average conifer tracheid (40 µm wide and 4 mm long; Panshin and de Zeeuw, 1980), an obliquely radial apoplastic pathway for water movement is plausible. By entering an axial tracheid through a bordered pit lower in the cell and exiting from the top into an adjacent cell, water could incrementally move closer to the cambium while encountering increased resistance in the latewood of each growth ring (discussed below). In this fashion, radial movement could occur in a roughly 1 : 100 (radial to axial) ratio, meaning that water could traverse 30 cm radially in a 30 m tree. Such a ratio is similar to diameter-to-height ratios in many tree species (i.e., 1 cm radial growth for 1 m of height growth) and could provide for sufficient radial water movement. It has also been shown in *Cryptomeria japonica* (Kitin et al., 2009) that the tips of tracheids are radially shifted such that individual tracheids from one tangential layer have common pit pairs with tracheids 2–3 layers closer to the cambium allowing for potential radial flow.

TABLE 4. Results of linear regression analysis using ray anatomy, ray tracheid (RT), and ray parenchyma (RP) characteristics, from outer sapwood samples, as independent variables and $k_{s\text{-}rad}$ as the dependent variable for Douglas-fir, ponderosa pine, and lodgepole pine. Regressions were fit to the linear model $y = \beta_1 a + \beta_2$ and considered significant at $P < 0.05$. Boldfaced values in rows indicate a significant relationship.

	Eastern sites				Western sites			
Character	β_1	β_2	P	R^2	β_1	β_2	P	R^2
Ponderosa pine								
Total ray lumen area (µm^2)	0.01	1.96	0.49	0.05	–0.04	4.57	0.32	0.10
RT average lumen area (µm^2)	–0.69	2.49	0.90	0.00	**-33.3**	**6.21**	**0.03**	**0.38**
RT cell frequency (no. mm^{-2})	0.01	1.73	0.44	0.06	–0.02	4.86	0.19	0.16
RT % of total area	9.01	2.24	0.76	0.01	**-245.1**	**5.24**	**0.01**	**0.47**
RP average lumen area (µm^2)	–0.94	2.66	0.87	0.00	–1.40	3.32	0.83	0.00
RP cell frequency (no. mm^{-2})	0.02	1.08	0.11	0.23	0.01	2.44	0.77	0.01
RP % of total area	42.43	1.64	0.22	0.15	0.89	2.92	0.99	0.00
Douglas-fir								
Total ray lumen area (µm^2)	–0.02	3.26	0.11	0.24	0.00	3.50	1.00	0.00
RT average lumen area (µm^2)	–10.98	2.94	0.18	0.17	1.40	3.39	0.92	0.00
RT cell frequency (no. mm^{-2})	**0.08**	**-3.18**	**0.03**	**0.40**	–0.01	3.80	0.85	0.00
RT % of total area	–164.4	2.92	0.22	0.15	3.40	19.27	0.92	0.00
RP average lumen area (µm^2)	–4.33	3.13	0.11	0.23	–0.15	3.49	0.94	0.00
RP cell frequency (no. mm^{-2})	4.98	180.92	0.72	0.01	0.00	3.21	0.85	0.00
RP % of total area	–0.01	0.06	0.11	0.23	–0.17	3.47	0.99	0.00
Lodgepole pine								
Total ray lumen area (µm^2)	0.02	1.72	0.35	0.09	0.00	3.04	0.83	0.00
RT average lumen area (µm^2)	0.13	2.85	0.98	0.00	–0.89	3.35	0.84	0.00
RT cell frequency (no. mm^{-2})	0.03	–0.34	0.27	0.12	–0.01	4.39	0.61	0.03
RT % of total area	14.16	2.51	0.74	0.01	–17.62	3.53	0.68	0.02
RP average lumen area (µm^2)	2.80	1.84	0.31	0.10	0.42	2.96	0.56	0.04
RP cell frequency (no. mm^{-2})	0.01	2.00	0.69	0.02	–0.02	4.45	0.24	0.14
RP % of total area	71.44	1.22	0.14	0.20	6.31	2.97	0.67	0.02

TABLE 5. Results of linear regression analysis using $k_{s\text{-}rad}$, of the outer sapwood samples, as the dependent variable and tree growth and physical characteristics of Douglas-fir, ponderosa pine, and lodgepole pine as independent variables. Regressions were fit to the linear model $y = \beta_1 a + \beta_2$ and considered significant at $P < 0.05$. Boldfaced values in rows indicate a significant relationship.

	Eastern sites				Western sites			
Character	β_1	β_2	P	R^2	β_1	β_2	P	R^2
Ponderosa pine								
Tree age (years)	–0.01	3.42	0.22	0.15	–0.02	3.99	0.69	0.02
Diameter at breast height (cm)	–0.03	3.61	0.48	0.05	–0.04	4.44	0.87	0.00
Sapwood depth (cm)	–0.02	2.60	0.90	0.00	0.04	2.45	0.81	0.01
Sapwood density ($g \cdot cm^{-3}$)	3.08	1.18	0.64	0.02	–8.14	6.80	0.19	0.17
No. growth rings in sample	0.02	2.15	0.47	0.05	**-0.33**	**4.58**	**0.01**	**0.48**
Mean annual growth rate (cm $year^{-1}$)	1.63	1.59	0.34	0.09	1.40	1.91	0.66	0.02
Douglas-fir								
Tree age (years)	2.13	96.62	0.59	0.03	–0.01	4.00	0.81	0.01
Diameter at breast height (cm)	0.00	1.74	0.61	0.03	–0.28	0.11	0.25	0.13
Sapwood depth (cm)	–0.02	2.33	0.96	0.00	0.09	3.24	0.78	0.01
Sapwood density ($g \cdot cm^{-3}$)	8.29	–1.80	0.11	0.23	13.45	–3.21	0.06	0.30
No. growth rings in sample	–0.05	2.86	0.32	0.10	–0.04	3.72	0.85	0.00
Mean annual growth rate ($cm \cdot year^{-1}$)	–5.80	4.43	0.37	0.08	3.44	1.54	0.34	0.09
Lodgepole pine								
Tree age (years)	0.00	2.99	0.95	0.00	–0.02	3.91	0.66	0.02
Diameter at breast height (cm)	0.00	2.93	0.98	0.00	–0.03	3.93	0.70	0.02
Sapwood depth (cm)	–0.19	3.86	0.20	0.16	–0.21	3.67	0.59	0.03
Sapwood density ($g \cdot cm^{-3}$)	–5.10	4.87	0.39	0.07	14.29	–2.64	0.28	0.12
No. growth rings in sample	0.10	1.91	0.40	0.07	–0.17	4.22	0.14	0.20
Mean annual growth rate ($cm \cdot year^{-1}$)	–0.28	2.98	0.96	0.00	0.04	3.14	0.99	0.00

Bordered pits on tangential walls of tracheids may comprise a fraction of the total area attributed to that of the ray cell lumen (Kitin et al., 2009) and offer a potential alternative apoplastic pathway to rays. However, because axial conductivity in latewood cells can be 11 times lower in Douglas-fir then compared to early wood (Domec and Gartner, 2002), this radial-oblique pathway is plausible but would encounter substantial resistance in the latewood. This diminished conductivity was evident in our dye tracer studies (Fig. 2D), which showed no dye flow into latewood tracheids from earlywood tracheids. However, it is possible that dynamic variation in hydraulic factors such as tension gradients will cause transient changes in radial pathways. Thus, the steady-state conditions used in this study may not have accurately replicated native conditions of radial tension. Future studies would greatly benefit from investigating combinations of pathways and tension gradients, then computing the relative conductances of the different pathways.

TABLE 6. Results of linear regression, with all species and ecotypes pooled together, using $k_{s\text{-}rad}$ as the dependent variable and ray and growth characteristics as independent variables. Regressions were tested from outer sapwood samples only. Regressions were fit to the linear model $y = \beta_1 a + \beta_2$ and considered significant at $P < 0.05$. Boldfaced values in rows indicate a significant relationship.

Character	β_1	β_2	P	R^2
Total ray lumen area (μm^2)	–0.68	52.35	0.82	0.01
Ray lumen % of total area	0.00	0.04	0.82	0.00
RT average lumen area (μm^2)	0.00	0.13	0.89	0.00
RT cell frequency ($no. \cdot mm^{-2}$)	–3.67	105.21	0.36	0.01
RT % of total area	–0.01	0.01	0.71	0.00
RP average lumen area (μm^2)	0.03	0.22	0.24	0.02
RP cell frequency ($no. \cdot mm^{-2}$)	–6.02	117.98	0.38	0.01
RP % of total area	0.00	0.02	0.97	0.00
Tree age (years)	**–8.83**	**95.26**	**0.003**	**0.12**
Diameter at breast height (cm)	**–1.48**	**38.67**	**0.029**	**0.07**
Sapwood depth (cm)	–0.99	9.21	0.10	0.04
Sapwood density ($g \cdot cm^{-3}$)	0.01	0.43	0.43	0.01
No. growth rings in sample	**-1.48**	**12.66**	**0.004**	**0.11**
Mean annual growth rate ($cm \cdot year^{-1}$)	**0.04**	**0.41**	**0.029**	**0.06**

Notes: RT = ray tracheid; RP = ray parenchyma

Year-to-year variations in ray development and trends in ray properties through the lifespan of a tree, add a further layer of complexity when attempting to elucidate relationships between anatomical and physiological characteristics. It is well established that rays originate at the vascular cambium from ray initials (Lev-Yadun and Aloni, 1995), but reports in the literature are contradictory with regard to the influence of environment and growth on the formation of rays or their anatomy (Bannan, 1937; Gregory and Romberger, 1975; Lev-Yadun, 1998; Gartner et al., 2000). Thus, it appears that year-to-year variations in both intrinsic and extrinsic factors affecting growth could affect the proportion and count of ray tracheids and ray parenchyma. This variation would make comparisons of $k_{s\text{-}rad}$ measurements from multiple-ring samples to anatomical images from an individual year's growth unreliable. Furthermore, inferences drawn from the cited studies may be constrained by an inability to clearly differentiate between ray tracheids and ray parenchyma. This difference is particularly important in species with higher proportions of ray tracheids (e.g., *Pinus* spp.; Hoadley, 1990; Denne and Turner, 2009) and may invalidate the assumption that ray anatomy parameters will be homogenous across multiple growth rings and, thus, a sample.

Despite the complexity of identifying radial pathways, there were significant and positive relationships between $k_{s\text{-}rad}$ and stem diameter, age and growth rate in our study (Table 5). These relationships provide evidence for a link between radial water transport and tree vigor. West-side trees of all species had higher growth rates (~50% higher; Table 2) and higher $k_{s\text{-}rad}$ (Table 3), but there were no significant relationships between $k_{s\text{-}rad}$ and growth (Table 5). Few other trends emerged in relation to the aridity gradient of our study design. This result is surprising given that previous records show significant differences in

hydraulic strategies over an aridity gradient (Maherali and DeLucia, 2000; Piñol and Sala, 2000; Barnard et al., 2011). Phloem has been hypothesized to play a role in diurnal refilling of embolized tracheids and vessels (e.g., Nardini et al., 2011), a process that may use ray parenchyma for storage and translocation of solutes and could possibly explain ecotype differences. However, further work is needed to clarify the relationship between stem ray parenchyma and xylem refilling.

Whereas radial water movement could be assumed to be important in overall tree hydraulics, little is known about the pathways—both apoplastic and symplastic—and thus about factors regulating radial flow. Perhaps the main role of direct radial conductivity is to supply the vascular cambium with sufficient water for cellular division and expansion. Nevertheless, more work is needed within individual growth rings, among several growth rings, and from studies of tree hydraulics investigated in vivo to improve our understanding of the dynamics of radial water movement. Rays make up an estimated 10–20% of total wood mass (Panshin and de Zeeuw, 1980), yet literature searches reveal a paucity of investigations into their structure and function. Although few relationships emerged between $k_{s\text{-}rad}$ and anatomical and morphological characteristics in our study, there can be little doubt that radial water movement does occur. Until this portion of the hydraulic pathway is better understood, a gap will remain in our understanding of how radial water movement contributes to whole-tree hydraulic function.

LITERATURE CITED

BAMBER, R. K. 1976. Heartwood, its function and formation. *Wood Science and Technology* 10: 1–8.

BANNAN, M. W. 1937. Observations on the distribution of xylem-ray tissue in conifers. *Annals of Botany* 1: 717–726.

BARNARD, D. M., F. C. MEINZER, B. LACHENBRUCH, K. A. MCCULLOH, D. M. JOHNSON, AND D. R. WOODRUFF. 2011. Climate-related trends in sapwood biophysical properties in two conifers: Avoidance of hydraulic dysfunction through coordinated adjustments in xylem efficiency, safety and capacitance. *Plant, Cell & Environment* 34: 643–654.

BURNS, R. M., AND B. H. HONKALA. 1990. Silvics of North America, vol. 1. Agricultural Handbook 654. USDA Forest Service, Washington, D.C., USA.

CHRISPEELS, M. J., AND C. MAUREL. 1994. Aquaporins: The molecular basis of facilitated water movement through living plant cells? *Plant Physiology* 105: 9–13.

COCHARD, H. 1992. Vulnerability of several conifers to air embolism. *Tree Physiology* 11: 73–83.

COTÉ, W. A., AND A. C. DAY. 1969. Wood ultra-structure of the southern yellow pines. Technical Publication No. 95, State University College of Forestry at Syracuse University, Syracuse, New York, USA.

DE BOER, A. H., AND V. VOLKOV. 2003. Logistics of water and salt transport through the plant: Structure and functioning of the xylem. *Plant, Cell & Environment* 26: 87–101.

DENNE, P., AND S. TURNER. 2009. Ray structure differences between root wood and stem wood in a range of softwood species. *International Association of Wood Anatomists Journal* 30: 71–80.

DOMEC, J.-C., AND B. L. GARTNER. 2002. How do water transport and water storage differ in coniferous earlywood and latewood? *Journal of Experimental Botany* 53: 2369–2379.

DOMEC, J.-C., F. C. MEINZER, B. L. GARTNER, AND D. R. WOODRUFF. 2006. Transpiration-induced axial and radial tension gradients in trunks of Douglas-fir trees. *Tree Physiology* 26: 275–284.

DOMEC, J.-C., M. L. PRUYN, AND B. L. GARTNER. 2005. Axial and radial profiles in conductivities, water storage and native embolism in trunks of young and old-growth ponderosa pine trees. *Plant, Cell & Environment* 28: 1103–1113.

FORD, C. R., C. E. GORANSON, R. J. MITCHELL, R. J. WILL, AND R. O. TESKEY. 2004a. Diurnal and seasonal variability in the radial distribution of sap flow: Predicting total stem flow in *Pinus taeda* trees. *Tree Physiology* 24: 951–960.

FORD, C. R., M. A. MCGUIRE, R. J. MITCHELL, AND R. O. TESKEY. 2004b. Assessing variation in the radial profile of sap flux density in *Pinus* species and its effect on daily water use. *Tree Physiology* 24: 241–249.

FUCHS, M., K. EHLERS, T. WILL, AND A. J. E. VAN BEL. 2010. Immunolocalization indicates plasmodesmatal trafficking of storage proteins during cambial reactivation in *Populus nigra. Annals of Botany* 106: 385–394.

GARTNER, B. L. 1995. Plant stems: Physiology and functional morphology. Academic Press, San Diego, California, USA.

GARTNER, B. L., D. C. BAKER, AND R. SPICER. 2000. Distribution and vitality of xylem rays in relation to tree leaf area in Douglas-fir. *International Association of Wood Anatomists Journal* 21: 389–401.

GARTNER, B. L., AND F. C. MEINZER. 2005. Structure–function relationships in sapwood water transport and storage. *In* M. Zwieniecki and N. M. Holbrook [eds.], Vascular transport in plants, 307–331. Elsevier Academic Press, Oxford, UK.

GORDON, M. 1912. Ray tracheids in *Sequoia sempervirens. New Phytologist* 11: 1–7.

GREGORY, R. A., AND J. A. ROMBERGER. 1975. Cambial activity and height of uniseriate vascular rays in conifers. *Botanical Gazette* 136: 246–253.

HOADLEY, R. B. 1990. Identifying wood: Accurate results with simple tools. Taunton Press, Newtown, Connecticut, USA.

JAMES, S. A., F. C. MEINZER, G. GOLDSTEIN, ET AL. 2003. Axial and radial water transport and internal water storage in tropical forest canopy trees. *Oecologia* 134: 37–45.

KITIN, P., T. FUJII, H. ABE, AND K. TAKATA. 2009. Anatomical features that facilitate radial flow across growth rings and from xylem to cambium in *Cryptomeria japonica. Annals of Botany* 103: 1145–1157.

KITIN, P., S. L. VOELKER, F. C. MEINZER, H. BEECKMAN, S. H. STRAUSS, AND B. LACHENBRUCH. 2010. Tyloses and phenolic deposits in xylem vessels impede water transport in low-lignin transgenic poplars: A study by cryo-fluorescence microscopy. *Plant Physiology* 154: 887–898.

KORAN, Z. 1977. Tangential pitting in black spruce tracheids. *Wood Science and Technology* 11: 115–123.

LAMING, P. B., AND P. B. H. WELLE. 1971. Anomalous tangential pitting in *Picea abies* Karst. (European spruce). *International Association of Wood Anatomists Journal* 4: 3–10.

LASSEN, L. E., AND E. A. OKKONEN. 1969. Sapwood thickness of Douglas-fir and five other western softwoods. U.S. Department of Agriculture, Forest Service Research Paper FPL-124, Forest Products Laboratory, Madison, Wisconsin, USA.

LEV-YADUN, S. 1998. The relationship between growth-ring width and ray density and ray height in cell number in the earlywood of *Pinus halpensis* and *Pinus pinea. International Association of Wood Anatomists Journal* 19: 131–139.

LEV-YADUN, S., AND R. ALONI. 1995. Differentiation of the ray system in woody plants. *Botanical Review* 61: 45–75.

LOVISOLO, C., AND A. SCHUBERT. 2006. Mercury hinders recovery of shoot hydraulic conductivity during grapevine rehydration: Evidence from a whole plant approach. *New Phytologist* 172: 469–478.

MACKAY, J. F. G., AND P. E. WEATHERLY. 1973. The effects of transverse cuts through the stems of transpiring woody plants on water transport and stress in the leaves. *Journal of Experimental Botany* 24: 15–28.

MAHERALI, H., AND E. H. DELUCIA. 2000. Xylem conductivity and vulnerability to cavitation of ponderosa pine growing in contrasting climates. *Tree Physiology* 20: 859–867.

MARK, W. R., AND D. L. CREWS. 1973. Heat-pulse velocity and bordered pit condition in living Engelmann spruce and lodgepole pine trees. *Forest Science* 19: 291–296.

MATON, C., AND B. L. GARTNER. 2005. Do gymnosperm needles pull water through the xylem produced in the same year as the needle? *American Journal of Botany* 92: 123–131.

NARDINI, A., M. A. LO GULLO, AND S. SALLEO. 2011. Refilling embolized xylem conduits: Is it a matter of phloem unloading? *Plant Science* 180: 604–611.

PANSHIN, A. J., AND C. DE ZEEUW. 1980. Textbook of wood technology. McGraw-Hill, New York, New York, USA.

PHILLIPS, N. R., R. OREN, AND M. ZIMMERMAN. 1996. Radial patterns of xylem sap flow in non-, diffuse- and ring-porous tree species. *Plant, Cell & Environment* 19: 983–990.

PIÑOL, J., AND A. SALA. 2000. Ecological implications of xylem cavitation for several Pinaceae in the Pacific Northwest. *Functional Ecology* 14: 538–545.

SANO, Y., Y. OKAMURA, AND Y. UTSUMI. 2005. Visualizing water-conduction pathways of living trees: Selection of dyes and tissue preparation methods. *Tree Physiology* 25: 269–275.

SAUTER, J. J., AND B. VAN CLEVE. 1994. Storage, mobilization and interrelations of starch, sugars, protein and fat in the ray storage tissue of poplar trees. *Trees* 8: 297–304.

SINGH, A. P., W. SCHMITT, R. MÖLLER, B. S. W. DAWSON, AND G. KOCH. 2006. Ray tracheids in *Pinus radiata* are more highly resistant to soft rot as compared to axial tracheids: Relationship to lignin concentration. *Wood Science and Technology* 40: 16–25.

SMITH, J. H. G., W. WALTERS, AND R. W. WELLWOOD. 1956. Variation in sapwood thickness of Douglas-fir in relation to tree and section characteristics. *Forest Science* 1: 97–103.

SPICER, R. 2005. Senescence in secondary xylem: Heartwood formation as an active developmental program. *In* M. Zwieniecki M. and N. M. Holbrook [eds.], Vascular transport in plants, 457–475. Elsevier Academic Press, Oxford, UK.

TYREE, M. T., B. SINCLAIR, P. LU, AND A. GRANIER. 1993. Whole shoot hydraulic resistance in *Quercus* species measured with a new high pressure flow meter. *Annals of Forest Science* 50: 417–423.

TYREE, M. T., AND M. H. ZIMMERMANN. 2002. Xylem structure and the ascent of sap. Springer, Berlin, Germany.

UMEBAYASHI, T., Y. UTSUMI, S. KOGA, S. INOUE, Y. SHIIBA, K. ARAKAWA, J. MATSUMURA, AND K. ODA. 2007. Optimal conditions for visualizing water conducting pathways in a living tree by the dye injection method. *Tree Physiology* 27: 993–999.

VAN BEL, A. J. E. 1990. Xylem-phloem exchange via the rays: The undervalued route of transport. *Journal of Experimental Botany* 41: 631–644.

YANG, S. D., AND M. T. TYREE. 1994. Hydraulic architecture of *Acer saccharum* and *A. rubrum*: Comparison of branches to whole trees and the contribution of leaves to hydraulic resistance. *Journal of Experimental Botany* 45: 179–186.